Pharmacological Research 158 (2020) 104871

Contents lists available at ScienceDirect

Pharmacological Research

journal homepage: www.elsevier.com/locate/yphrs

Imperatorin alleviates cancer cachexia and prevents muscle wasting via directly inhibiting STAT3

Linlin Chen[a,b,1], Weiheng Xu[c,1], Quanjun Yang[a], Hong Zhang[a,b], Lili Wan[a], Bo Xin[a], Junping Zhang[c,d,**], Cheng Guo[a,b,*]

[a] Department of Pharmacy, Shanghai Jiao Tong University Affiliated Sixth People's Hospital, Shanghai 200233, PR China
[b] School of Medicine, Shanghai Jiao Tong University, Shanghai 200240, PR China
[c] School of Pharmacy, Second Military Medical University, Shanghai 200433, PR China
[d] College of Pharmacy, Fujian University of Traditional Chinese Medicine, Fuzhou, Fujian 350122, PR China

ARTICLE INFO

Keywords:
Cancer cachexia
Skeletal muscle wasting
STAT3
Imperatorin
Muscle degradation
E3 Ubiquitin ligases

ABSTRACT

Skeletal muscle wasting is the most remarkable phenotypic feature of cancer cachexia that increases the risk of morbidity and mortality. Imperatorin (IMP), a main bioactive component of *Angelica dahurica* Radix, has been reported to possess several pharmacological effects including potential anti-colitis, anti-arthritis and anti-tumor activities. In this work, we demonstrated that IMP is a promising agent for the treatment of muscle wasting in cancer cachexia. IMP (5 − 20 μM) dose-dependently attenuated TCM-induced C2C12 myotube atrophy and prevented the induction of E3 ubiquitin ligases muscle RING-finger containing protein-1 (MuRF1) and muscle atrophy Fbox protein (Atrogin-1/MAFbx). Moreove, IMP administration significantly improved chief features of cancer cachexia *in vivo*, with significant prevention of the loss of body weight and deleterious wasting of multiple tissues, including skeletal muscle, fat and kidney and decreased expression of MuRF1 and Atrogin-1 in cachectic muscles. Cellular signaling pathway analysis showed that IMP selectively inhibited the phosphorylation of signal transducer and activator of transcription 3 (STAT3) *in vitro* and *in vivo*, and surface plasmon resonance (SPR) affinity experiments further demonstrated IMP bound to STAT3 in a concentration-dependent resonance manner. Molecular docking results revealed that IMP binds to the SH2 domain of STAT3, forming a hydrogen bond interaction with Arg-609, and a Sigma-Pi interaction with Lys-591. Mechanism analysis demonstrated that STAT3 overexpression markedly weakens the improvements of IMP on myotube atrophy and muscle wasting of cancer cachexia, indicating that STAT3 mediated the therapeutic effect of IMP. All these favorable results indicated that IMP is a new potential therapeutic candidate for cancer cachexia.

1. Introduction

Cancer cachexia is a complex multifactorial syndrome characterized by the ongoing loss of body weight and skeletal muscle mass [1]. Depletion of skeletal muscle is recognized as an independent predictor of mortality and is associated with functional impairment, poor quality of life and less tolerance and response to anticancer therapies [2–4]. Reversal of muscle loss in animal models of cancer cachexia leads to prolongation of survival and maintaining muscle mass represents a major goal in the treatment of cancer patients [5,6]. However, therapeutic strategies progress slowly and discovery of new drugs for cancer cachexia is needed [7–9].

Loss of skeletal muscle mass is associated with activation of several signaling pathways or mediators, including signal transducer and

Abbreviation: Atrogin-1/MAFbx, muscle atrophy Fbox protein; CMC-Na, carboxymethyl cellulose sodium; CSA, myofiber cross-section areas; DAPI4, 6-diamidino-2-phenylindole; FOXO3, forkhead box protein O3; IMP, Imperatorin; JAK, Janus kinase; MuRF1, muscle RING-finger containing protein-1; MyHC, myosin heavy chain; NF-κB, nuclear factor-kappa B; SH2, Src homology 2; SMAD, small mothers against decapentaplegic homolog; SPR, surface plasmon resonance; STAT3, signal transducer and activator of transcription 3; TCM, colon adenocarcinoma CT26 conditioned medium

* Corresponding author at: Department of Pharmacy, Shanghai Jiao Tong University Affiliated Sixth People's Hospital, 600#, Yishan Road, Shanghai, 200233, PR China.
** Corresponding author at: School of Pharmacy, Second Military Medical University, 325#, Guohe Road, Shanghai 200433, PR China.
E-mail addresses: llchen1015@163.com (L. Chen), xuweiheng7114@163.com (W. Xu), myotime@sjtu.edu.cn (Q. Yang), edwardzh@sjtu.edu.cn (H. Zhang), wanlily3533@163.com (L. Wan), jiayouxinbo@126.com (B. Xin), jpzhang08@163.com (J. Zhang), guopharm@126.com (C. Guo).
[1] These authors contributed equally to this work.

https://doi.org/10.1016/j.phrs.2020.104871
Received 7 January 2020; Received in revised form 9 April 2020; Accepted 24 April 2020
Available online 12 May 2020

activator of transcription 3 (STAT3) [10–12], nuclear factor-kappa B (NF-κB) [13–15], small mothers against decapentaplegic homolog 2/3 (SMAD2/3) [16,17] and forkhead box protein O3 (FOXO3) [18,19]. Pro-inflammatory cytokines derived from immune or tumor cells in cancer cachexia, including tumor necrosis factor-α (TNF-α), interleukin-1 (IL-1) and interleukin-6 (IL-6) have been shown to trigger muscle wasting [2,20], through activation of the NF-κB and janus kinase-signal transducer and activator of transcription (JAK-STAT) pathways [11,21], respectively. Transforming growth factor beta (TGFβ) superfamily ligands including myostatin and activin can activate SMAD2 and SMAD3, which together with the common mediator, SMAD4, translocate to the nucleus and regulate transcriptional responses leading to muscle wasting [16,22]. Additionally, transcription factor FOXO3 is also significantly associated with body weight and muscle mass loss [18]. The activation of these signaling pathways allows for the increased transcription of genes encoding E3 ubiquitin ligases muscle RING-finger protein-1 (MuRF1) and muscle atrophy Fbox protein (Atrogin-1/MAFbx) that are involved in muscle protein degradation [23–25].

Imperatorin is a naturally occurring furanocoumarin isolated from *Angelica dahurica* Radix, and possesses several pharmacological activities such as anti-colitis, anti-arthritis and anti-tumor [26–29]. In this study, we mainly investigated the therapeutic effect of IMP on cancer cachexia and explored the possible mechanisms. We found that IMP could reverse myotube atrophy and inhibit MuRF1 and Atrogin-1 expression *in vitro*. Importantly, IMP could also alleviate cancer cachexia and prevent muscle wasting *in vivo*. Further investigations revealed that IMP specifically inhibited STAT3 phosphorylation via directly binding to the SH2 domain of STAT3 and overexpression of STAT3 drastically weakened the efficacy of IMP, suggesting that the therapeutic effect of IMP can be attributed to directly inhibiting STAT3. These findings provide novel insights into the anti-cachexia effect of IMP, which may be a promising drug candidate for treatment of cancer cachexia.

2. Materials and methods

2.1. Reagents and antibodies

Antibodies against p-STAT3 (Yyr705) (#9145), STAT3 (#9139), p-NF-κB (Ser536) (#3033), NF-κB (#8242), p-SMAD3 (Ser423/425) (#9520), SMAD3 (#9523), p-STAT1 (Tyr701) (#9167), STAT1 (#9172), p-JAK2 (Tyr1007/1008) (#3776), JAK2 (#3230), GAPDH (#5174), Alexa Fluor® 488 conjugate (#4408S) IgG and Alexa Fluor® 594 conjugate (#8889S) IgG were obtained from Cell Signaling Technology (Beverly, MA); antibodies against p-FOXO3 (sc-101683) and FOXO3 (sc-48348) were obtained from Santa Cruz Biotechnology; antibodies against MuRF1 (ab172479), Atrogin-1 (ab168372) and recombinant human protein STAT3 (ab43618) were purchased from Abcam (Cambridge, MA); antibody against myosin heavy chain (MyHC, MAB4470) was obtained from R&D Systems (Minneapolis, MN); antibodies against IRDye 800CW (926–32210 and 926–32211) were purchased from LICOR (Lincoln, Nebraska). Imperatorin (IMP) was obtained from Efebio (Shanghai, China).

2.2. Cell cultures

Murine C2C12 myoblasts, human Hela and HEK293 T cell lines (Cell Bank of Shanghai Branch, Chinese Academy of Sciences) were cultured in DMEM (Corning Life Sciences, NY, USA) supplemented with 10 % fetal bovine serum (FBS, Gibco, MA, USA) and 1% penicillin/streptomycin. Murine CT26 colon adenocarcinoma cells (CRL-2638, ATCC) were cultured in RPMI-1640 medium (Corning Life Sciences, NY, USA) supplemented with 10 % FBS and 1% penicillin/streptomycin. To induce myotube formation, C2C12 myoblasts were grown to 90 % confluence and changed to DMEM with 2% horse serum (Gibco, MA, USA) for 3 days. We found that myotubes generated from early passage C2C12 myoblast cells (< 10 passages) yielded most consistent results.

2.3. The conditioned medium collection

CT26 colon adenocarcinoma cells (2×10^6 cells) were seeded in 10 mm dishes and grown to 90 % confluence. The medium was changed to DMEM with 2% horse serum medium for 36 h and cell supernatant was collected and centrifuged at 450×g for 5 min. The supernatant was referred to as tumor conditioned medium (TCM).

2.4. Immunofluorescence

C2C12 myotubes were fixed in 4% paraformaldehyde and permeabilized with 0.5 % Triton X-100 at room temperature, followed by incubation with MyHC antibody or a mixture of MyHC and p-STAT3 antibodies overnight at 4°C. After incubating with secondary antibodies, C2C12 myotubes were then stained with 10 μg/mL 4, 6-diamidino-2-phenylindole (DAPI, Sigma-Aldrich, St Louis, USA), and photographed using Cellsens software (Olympus Corporation, Tokyo, Japan).

2.5. Animal experimentation

All animal care and experiments were conducted according to the guidance of China Animal Welfare Legislation, and approved by the Ethics on Animal Care and Treatment Committee of Shanghai Jiao tong University. Healthy male Balb/c mice, 6—8 weeks old, were purchased from the SLAC Laboratory Animal Co. Ltd (Shanghai, China). The animals were maintained at a constant temperature and humidity with a 12:12 h dark/light cycle.

The mouse model of cancer cachexia was established as previously described [30,31]. Briefly, Balb/c mice were injected with CT26 cells (2×10^6 cells/200 μL) into the right flank subcutaneously, and then randomly divided into four groups (n = 10 per group). Mice received daily oral gavage of 25 or 50 mg/kg/day of IMP diluted in 0.5 % carboxymethyl cellulose sodium (CMC-Na) solvent or solvent as a control beginning at 15 days after tumor inoculation. Dose selection of IMP was based on models of xenograft tumor (50 and 100 mg/kg) [32] and inflammatory bowel disease (25, 50 and 100 mg/kg) [26]. The body weights, food intake and tumor weights were measured every two days. Tumor weights (mg) were computed using the formula: 0.52 × tumor length × tumor width [2]. After 15 days of treatment, mice were sacrificed after exposure to CO_2, and the weights of tumors, muscles and organs (epididymal fat, kidney and heart) were then determined. Some muscles were quickly frozen in liquid nitrogen and the remaining were fixed in 4% polyformaldehyde for subsequent analysis.

2.6. Histological examination

Gastrocnemius muscles were fixed with 4% paraformaldehyde and embedded in paraffin. The myofiber sizes were measured in sections stained with haematoxylin-eosin (H&E) and analyzed using Cellsens software. The myofiber cross-section areas (CSA) were determined from approximately 180 myofibers per group. Immunofluorescence staining was conducted to detect the expression of MyHC and MuRF1 and immunohistochemical examination was performed to analyze p-STAT3 positive staining of cell nuclei.

2.7. Western blot analysis

C2C12 myotubes and muscle samples were lysed using RIPA buffer (Thermo Fisher Scientific, MA, USA) containing Protease Inhibitor and Phosphatase Inhibitor Cocktail (Yeasen, Shanghai, China). After centrifugation (12,000 rpm, 10 min, 4°C), proteins were separated on 10 % sodium dodecyl sulfate polyacrylamide gel, and transferred onto nitrocellulose membranes (Millipore Corporation, Bedford, USA). The

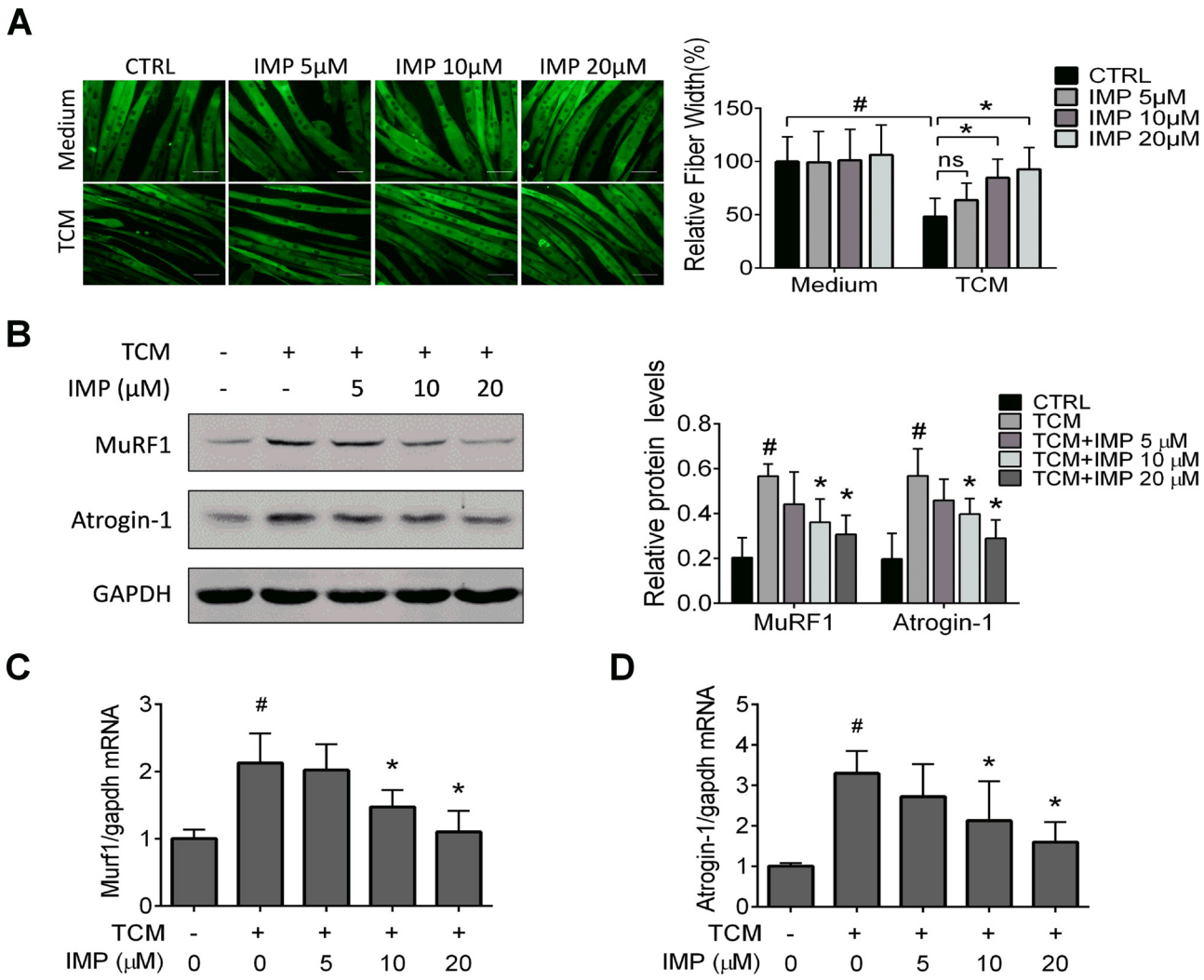

Fig. 1. IMP attenuates myotube atrophy induced by TCM. (A) C2C12 myotubes were pretreated with IMP for 2 h and then stimulated by TCM for 72 h. Representative images of immunofluorescence staining for MyHC (green) are shown (left panel). Scale bars =50 μm. The fiber widths of each experiment were measured and calculated (right panel). n > 150 per group. $^{\#}P < 0.05$ versus untreated control, $^{*}P < 0.05$ versus TCM control. (B) C2C12 myotubes were pretreated with IMP for 2 h and then stimulated by TCM for 48 h. The expression of indicated proteins was determined by western blot. The band intensities were quantified and GAPDH was used as control. n = 3. $^{\#}P < 0.05$ versus untreated control, $^{*}P < 0.05$ versus TCM control. (C and D) C2C12 myotubes were pretreated with IMP for 2 h and then stimulated by TCM for 24 h. mRNA levels of *Murf1* (C) and *Atrogin-1* (D) were analyzed by real-time PCR and normalized to *Gapdh*. n = 3. $^{\#}P < 0.05$ versus untreated control, $^{*}P < 0.05$ versus TCM control.

membranes were incubated with primary antibodies overnight at 4 ˚C, followed by incubation with secondary antibodies at room temperature for 1 h, and then visualized using Odyssey system (LICOR, Lincoln, Nebraska). The density of each band of proteins was quantified by ImageJ Software.

2.8. Quantitative PCR (qPCR)

Total RNA was isolated from C2C12 myotubes and muscle samples using RNAiso reagent (Takara, Otsu, Japan), and one microgram of total RNA was reverse transcribed into cDNA using Primescipt II RT Master Mix Kits (Takara, Otsu, Japan) according to manufacturer's protocol. Samples were diluted 1/20 and used to evaluate the mRNA expression of *Murf1* and *Atrogin-1*. These genes were normalized to reference gene glyceraldehyde 3-phosphate dehydrogenase (*Gapdh*), and the relative expressions were calculated using ΔΔCt method. Primer sequences for detection of mRNA are following: *Murf1* Forward: 5′-AGTGTCCATGTCTGGAGGTCGTTT-3′, *Murf1* Reverse: 5′-ACTGGAG CACTCCTGCTTGTAGAT-3′, *Atrogin-1* Forward: 5′-ACGTCGCAGCCAA GAAGAG-3′, *Atrogin-1* Reverse: 5′-ATGGCGCTCCTTCGTACTTC-3′, *Gapdh* Forward: 5′-GGGTGTGAACCACGAGAAAT-3′, *Gapdh* Reverse: 5′-CCTTCCACAATGCCAAAGTT-3′.

2.9. STAT3 luciferase reporter assay

HeLa cells were infected with viral vectors bearing a luciferase reporter gene driven by STAT3 promoter (Genomeditech, Shanghai, China) and then incubated with 8 ng/mL blastincidin (Solarbio, Beijing, China) for 7–8 days. After screening by blastincidin, HeLa cells were transfected with pRL-SV40 plasmid (Beyotime, Haimen, China) using FuGENE® HD (Promega, Madison, USA) and then incubated with IMP (5 − 20 μM) for 4 h, followed by TCM stimulation for another 24 h. The expression of luciferase was detected by Dual Luciferase Reporter Assay kits (Promega, Madison, USA). All luciferase experiments were repeated three times.

2.10. Surface plasmon resonance assay and molecular docking

Surface plasmon resonance (SPR) assays were performed with Biacore T200 system as previously described [33]. Briefly, the GST

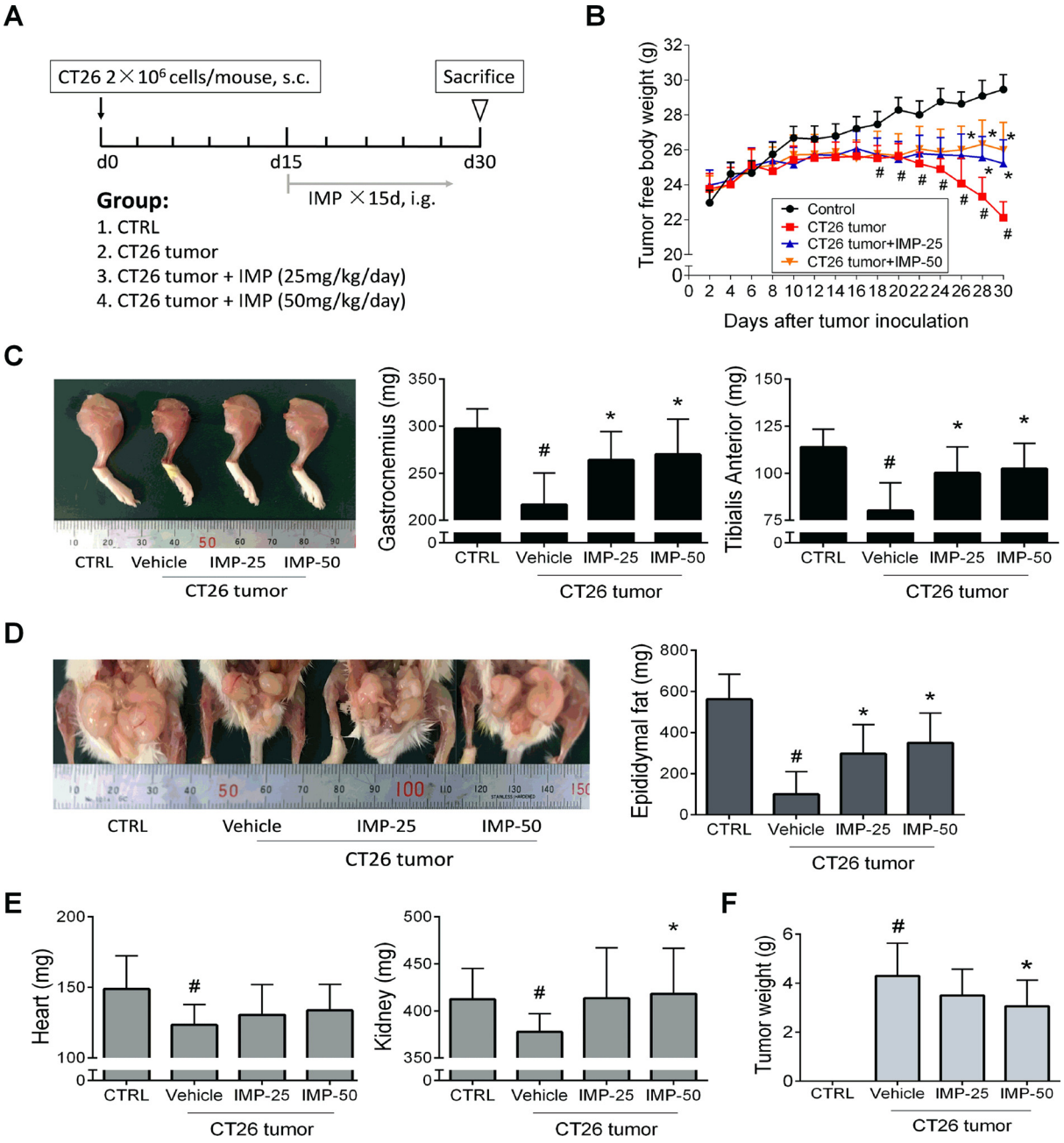

Fig. 2. IMP prevents cancer cachexia in CT26 tumor-bearing mice. (A) Schematic representation of experimental design. CT26 tumor cells were implanted s.c. in the right flank of mice on day 0 and IMP (25, 50 mg/kg/day) were orally administrated starting on day 15 after tumor inoculation. Healthy control and vehicle control received equal volume of solvent. The effects of IMP on the main features of cachexia were examined, including (B) tumor free body weight, (C) gastrocnemius and tibialis anterior muscles mass, (D) epididymal fat mass, (E) kidney and heart mass and (F) tumor weigh. n = 10 mice/group. $^{\#}P < 0.05$ versus healthy control, $^{*}P < 0.05$ versus vehicle control.

tagged-recombinant STAT3 protein was diluted in 10 mM sodium acetate (pH = 4.0, 20 μg/mL) and then immobilized on the CM5 chip (GE Healthcare, Sweden) for 10 min. Different concentrations of IMP (0.125–32 μM) were injected at a flow rate of 30 μL/min to pass through the surface of STAT3-immobilized CM5 chip. The interaction mode and kinetic constant of IMP with STAT3 were obtained from 1:1 kinetic model in Biacore T200 evaluation software (GE Healthcare, Sweden). Molecular docking was performed by employing the CDOCKER module in the DS 3.0 package. The crystal structure of STAT3 protein was downloaded from the Protein Data Bank (PDB ID: 1BG1) [34]. Prior to docking, DNA chain and water molecules were removed. The docking site was defined at the Src homology 2 (SH2) domain (coordinates: 103.03, 55.64, 0.25) of STAT3, with a radius of 15 Å. IMP was docked into the defined catalytic site, and the top hits, random conformation and orientations to refine were set as 10. The other options were set as default settings.

2.11. *Lentivirus production and transfection*

To prepare lentiviruses expressing STAT3 or GFP, HEK293 T cells were co-transfected with 4 μg STAT3 or GFP lentiviral vector plasmids (Genomeditech, Shanghai, China) plus 3 μg pSPAX2 and 1 μg pMD2.G using FuGENE® HD. Virus particles were concentrated using PEG8000 according to the manufacturer's instructions. *in vitro*, C2C12 myotubes were transfected with lentiviruses and protein expressions were detected by western blot after 96 h. *in vivo*, lentiviruses expressing STAT3

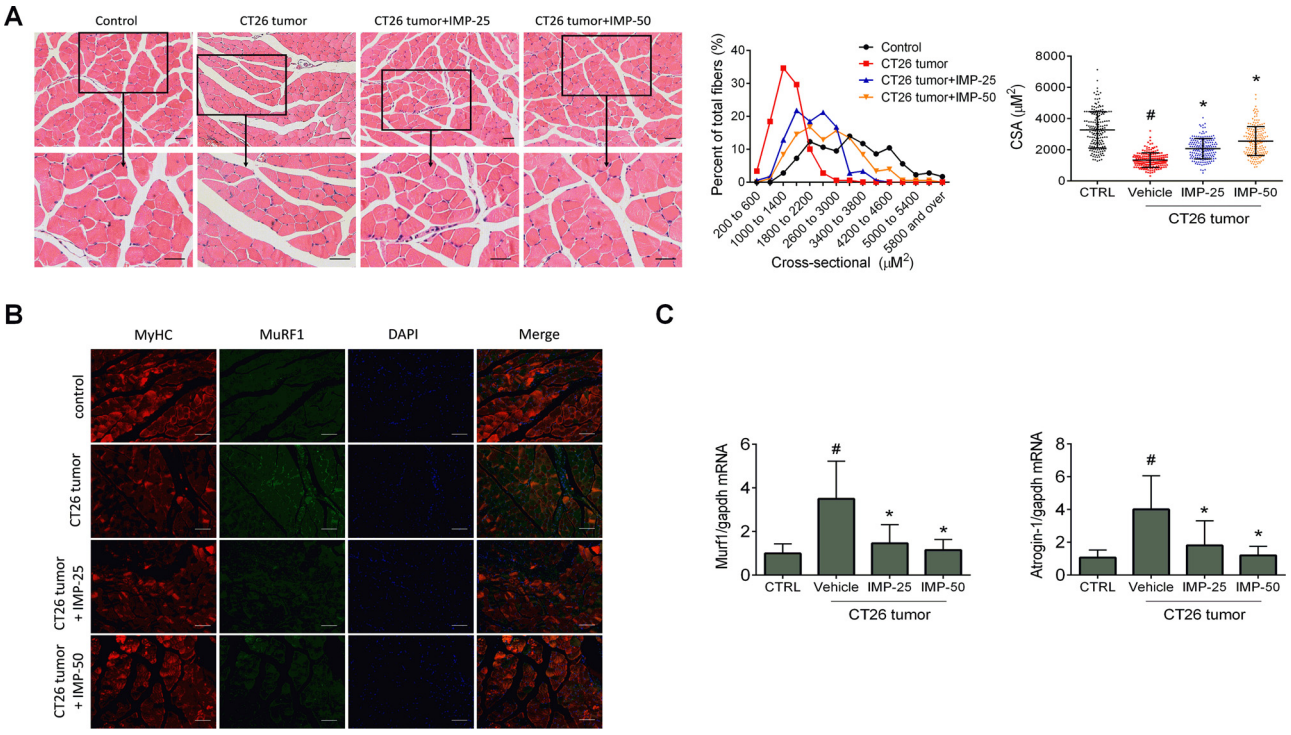

Fig. 3. IMP ameliorates muscle wasting in CT26 tumor-bearing mice. (A) Gastrocnemius muscle was observed histologically by H&E staining. Scale bars = 50 μm. The cross-sectional areas of approximately 180 myofibers per group were determined. n = 3 mice/group. $^{\#}P < 0.05$ versus healthy control, $^{*}P < 0.05$ versus vehicle control. (B) Immunofluorescence staining was carried out to detect the expression of MyHC (red) and MuRF1 (green). Scale bars = 100 μm. (C) mRNA levels of *Murf1* and *Atrogin-1* in gastrocnemius muscles were analyzed by real-time PCR and normalized to *Gapdh*. n = 10 mice/group. $^{\#}P < 0.05$ versus healthy control, $^{*}P < 0.05$ versus vehicle control.

were injected into right hindlimb of 5 weeks old male Balb/c mice, and lentiviruses expressing GFP were injected into the left hindlimb as control. One week later, the lentiviruses were injected repeatedly and mice were randomly divided into three groups (n = 10 per group): control group, CT26 tumor group and IMP (50 mg/kg/day) treatment group. The mouse model of cancer cachexia was established as above.

2.12. Statistical analysis

Results are presented as mean ± SD and were analyzed by analysis of variance (ANOVA) followed by paired comparison, as appropriate. Differences were considered statistically significant at $P < 0.05$.

3. Results

3.1. IMP attenuates myotube atrophy induced by TCM

Muscle wasting is a key manifestation of cancer cachexia. To explore the anti-cachexia effect of IMP, we initially evaluated its effect on myotube atrophy using C2C12 myotube model. Results showed that IMP (5 − 20 μM) dose-dependently reversed myotube atrophy induced by TCM, as assessed by morphological changes and myotube fiber width (Fig. 1A). In addition, TCM-induced expression of MuRF1 and Atrogin-1 mRNA and protein was drastically inhibited by IMP (Fig. 1B-D). These effects were not attributed to its cytotoxicity as cell cytotoxicity was not observed at concentrations below 30 μM (Fig. S1).

3.2. IMP prevents cancer cachexia and improves muscle wasting in CT26 tumor-bearing mice

We next evaluated the anti-cachexia effect of IMP in an experimental model of cancer cachexia using CT26 colorectal adenocarcinoma (Fig. 2A). CT26 tumor-bearing mice showed a progressive loss of body mass beginning on day 18 after tumor inoculation (Fig. 2B). Moreover, weights of gastrocnemius, tibialis anterior muscles and epididymal fat as well as heart and kidney mass were strikingly decreased in tumor-bearing mice when mice were killed on day 30 (Fig. 2C-E). IMP administration distinctly improved chief features of cancer cachexia in a dose-dependent manner, with significant prevention of the loss of body weight, gastrocnemius muscle mass, tibialis anterior muscle mass and epididymal fat mass (Fig. 2B-D). Additionally, IMP treatment improved kidney mass and this effect reached statistically significance at dose of 50 mg/kg (Fig. 2E). Meanwhile, IMP (50 mg/kg) also showed a significant inhibition on tumor growth (Fig. 2F).

Histological examination of gastrocnemius muscles showed that IMP significantly increased the sizes of myofibers in a dose dependent manner (Fig. 3A). As evidenced by immunofluorescence staining, IMP administration induced an apparent reduction of MuRF1 expression, accompanied with an increase of MyHC in tibialis anterior muscle (Fig. 3B). Moreover, *Murf1* and *Atrogin-1* mRNA levels were also dose dependently inhibited by IMP (Fig. 3C). These data indicate that IMP has therapeutic effect on cancer cachexia and ameliorates muscle wasting in CT26 tumor-bearing mice.

3.3. IMP inhibits STAT3 pathway

To investigate the possible mechanisms underlying the anti-cachexia effect of IMP, we examined the alterations of intracellular signaling pathways related to muscle wasting. Results showed that IMP specifically suppressed the phosphorylation of STAT3 and expression of its down-stream target gene C/EBPδ in C2C12 myotube atrophy model, but had no effect on NF-κB, SMAD3 and FOXO3 (Fig. 4A). As shown by immunofluorescence staining, IMP also exhibited an inhibitory effect on nuclear translocation of p-STAT3 (Fig. 4B). Moreover, the transcriptional activity of STAT3 was suppressed as well (Fig. 4C). Furthermore, we also tested the inhibitory effect of IMP on IL-6-induced

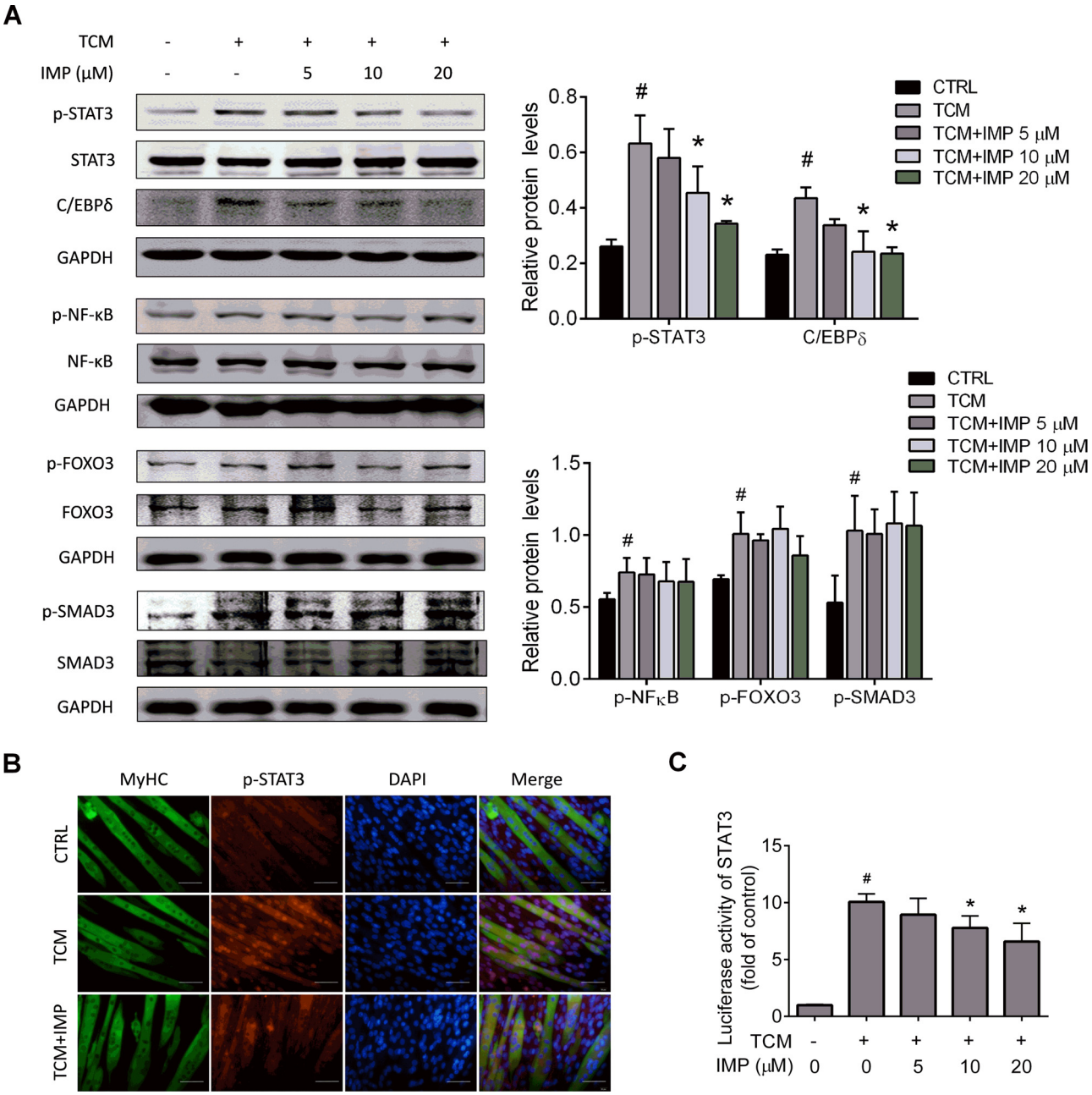

Fig. 4. IMP inhibits STAT3 signaling pathway in TCM-induced myotube atrophy. (A) C2C12 myotubes were pretreated with IMP (5-20 μM) for 2 h and then stimulated by TCM for 48 h. The expression of indicated proteins was determined by western blot. The band intensities were quantified and GAPDH or the non-phosphorylated protein forms were used as control. n = 3. $^{\#}P < 0.05$ versus untreated control, $^{*}P < 0.05$ versus TCM control. (B) C2C12 myotubes were pretreated with IMP (20 μM) for 2 h and then stimulated by TCM for 30 min. Representative images of immunofluorescence staining for MyHC (green), p-STAT3 (red) and DAPI (blue) are shown. Scale bar =50 μm. (C) HeLa cells were transfected with viral vectors bearing a luciferase reporter gene driven by STAT3 promoter and pRL-SV40 plasmids and then stimulated by TCM for 24 h in the presence of different concentrations of IMP (5-20 μM). Luciferase activity was measured using a dual-luciferase reporter assay kit. n = 3. $^{\#}P < 0.05$ versus untreated control, $^{*}P < 0.05$ versus TCM control.

STAT3 activation and obtained similar results (Fig. S2). Consistent with cellular data, IMP administration also inhibited STAT3 phosphorylation in gastrocnemius muscles of CT26 tumor-bearing mice as shown by western-blot and immunohistochemical staining (Fig. 5A and B), which further confirmed that IMP specifically inhibited STAT3 pathway.

3.4. IMP directly binds to SH2 domain of STAT3

Activation of JAKs mediates tyrosine phosphorylation of STAT3, followed by their dimerization, nuclear translocation, and activation of target genes. In order to identify the direct target of IMP, we examined its effect on phosphorylation of JAK2 and STAT1. The results showed that IMP had no impact on their phosphorylation, suggesting that IMP may directly interact with STAT3 itself (Fig. 6A). To confirm this possibility, SPR affinity experiments were conducted to assess the STAT3-binding activity of IMP. In accordance with our expectation, IMP (0.125−32 μM) showed specific binding activity to STAT3 in a concentration-dependent resonance manner with maximum response at 9.59 RU (Fig. 6B). The Kd was computed to be 9.98 μM (Chi^2 = 0.448 RU^2) (Fig. 6C). Then molecular docking was performed to predict specific binding mode within the active site of STAT3 by CDOCER in DS 3.0 and results demonstrated that IMP bound to the SH2 domain of

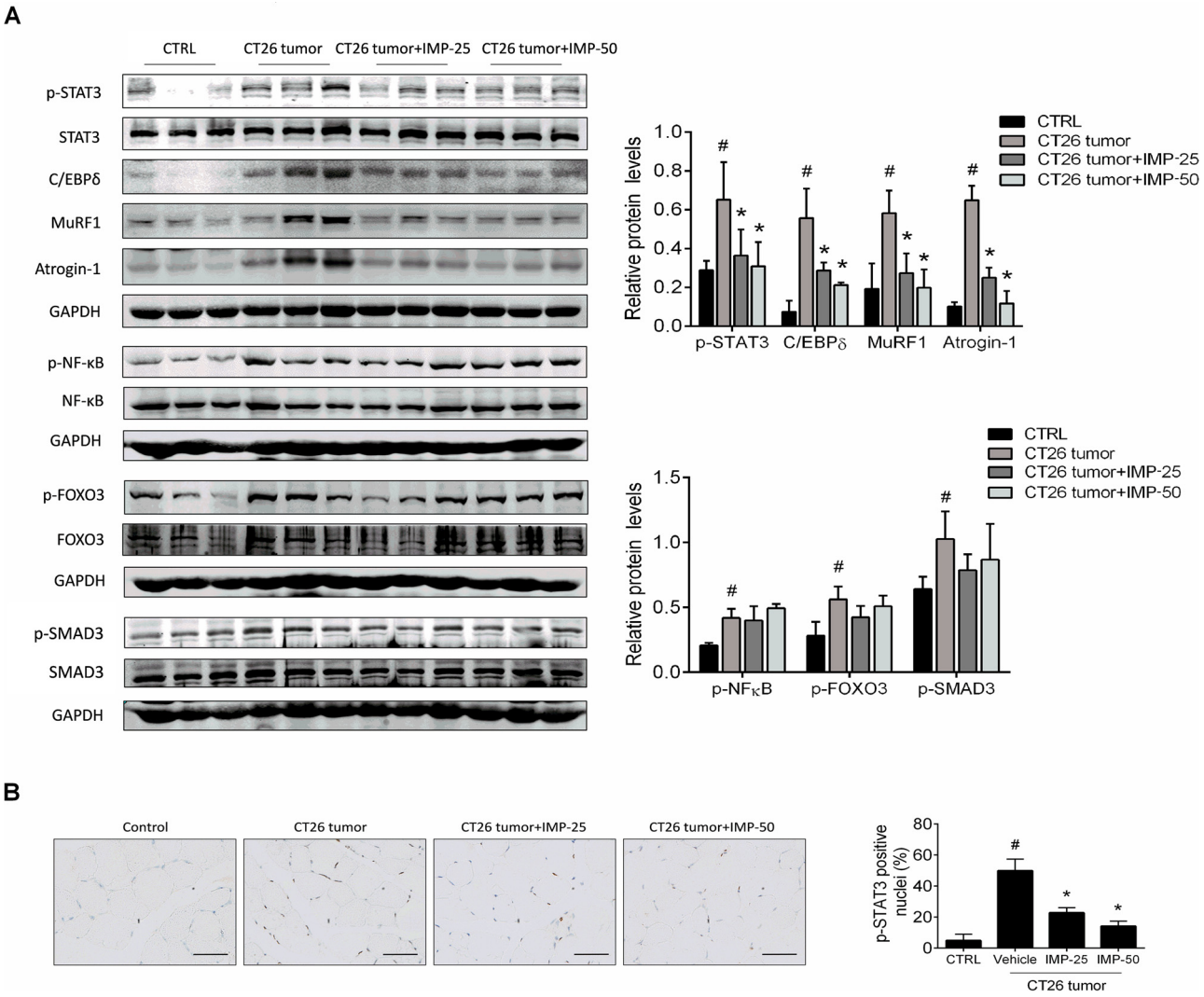

Fig. 5. IMP inhibits STAT3 signaling pathway in muscles of CT26 tumor-bearing mice. (A) The expression of indicated proteins in gastrocnemius muscles was detected by western blot. The band intensities were quantified and GAPDH or the non-phosphorylated protein forms were used as control. n = 3 mice/group. $^{\#}P < 0.05$ versus healthy control, $^{*}P < 0.05$ versus vehicle control. (B) Representative images of immunohistochemical staining for p-STAT3 in gastrocnemius muscle sections (left panel). Scale bar =50 μm. The percentage of p-STAT3-positive cell nuclei in a total of 350 nuclei was counted manually (right panel). n = 3 mice/group. $^{\#}P < 0.05$ versus healthy control, $^{*}P < 0.05$ versus vehicle control.

STAT3 with a binding energy of - 4.7689 kJ/mol (Fig. 6D). IMP forms a hydrogen bond interaction with Arg-609, and forms a Sigma-Pi interaction with Lys-591. In addition, IMP can interact with Glu-594, Arg-595, Ile-634, Gln-635, Ser-636, Val-637, Glu-638, Pro-639, Thr-620, Ser-611, Ser-612, Ser-613 and other amino acid residues to form intermolecular hydrophobic interaction (Fig. 6E).

3.5. IMP improves muscle wasting through STAT3 inhibition

To investigate whether STAT3 inhibition mediated the therapeutic effect of IMP on cancer cachexia, we conducted experiments to overexpress STAT3 and evaluate its effects on myotube atrophy *in vitro*. Overexpression of STAT3 resulted in a significant reduction in fiber diammer and marked myotube atrophy compared with GFP group. IMP treatment almost completely reversed myotube atrophy induced by TCM in GFP group, but the improvement was greatly weakened in STAT3 overexpression group, (~30 % improvement of myotube atrophy in STAT3 overexpression group and ~88 % in GFP group, Fig. 7A). Moreover, overexpression of STAT3 also weakened the inhibitory effect of IMP on Atrogin-1 expression (Fig. 7B).

To further confirm the mediating effect of STAT3, gastrocnemius muscles of the mice were infected with lentiviruses to overexpress STAT3 and anti-cachexia effect of IMP was then evaluated. The schematic representation of experimental design was shown in Fig. S3. Our results demonstrated that IMP had a great improvement on muscle wasting in GFP group, but its anti-cachexia effect was slightly weakened in STAT3 overexpression group as evidenced by gastrocnemius muscle mass, HE staining and cross-sectional area analysis (~45 % improvement of myofiber atrophy in STAT3 overexpression group and ~63 % in GFP group, Fig. 8A and B). Moreover, the inhibitory effect of IMP on Atrogin-1 expression in gastrocnemius muscle also slightly weakened after STAT3 overexpression (Fig. 8C). Overall, these data demonstrated that STAT3 mediated the anti-cachexia effect of IMP.

4. Discussion

In this study, we demonstrated that IMP attenuated myotube atrophy in C2C12 myotube model and alleviated cancer cachexia in CT26 tumor-bearing mice. Investigation of the molecular mechanisms revealed that IMP specifically inhibited STAT3 phosphorylation through directly binding to SH2 domain of STAT3. Because of significantly diminished efficacy of IMP after STAT3 overexpression, we

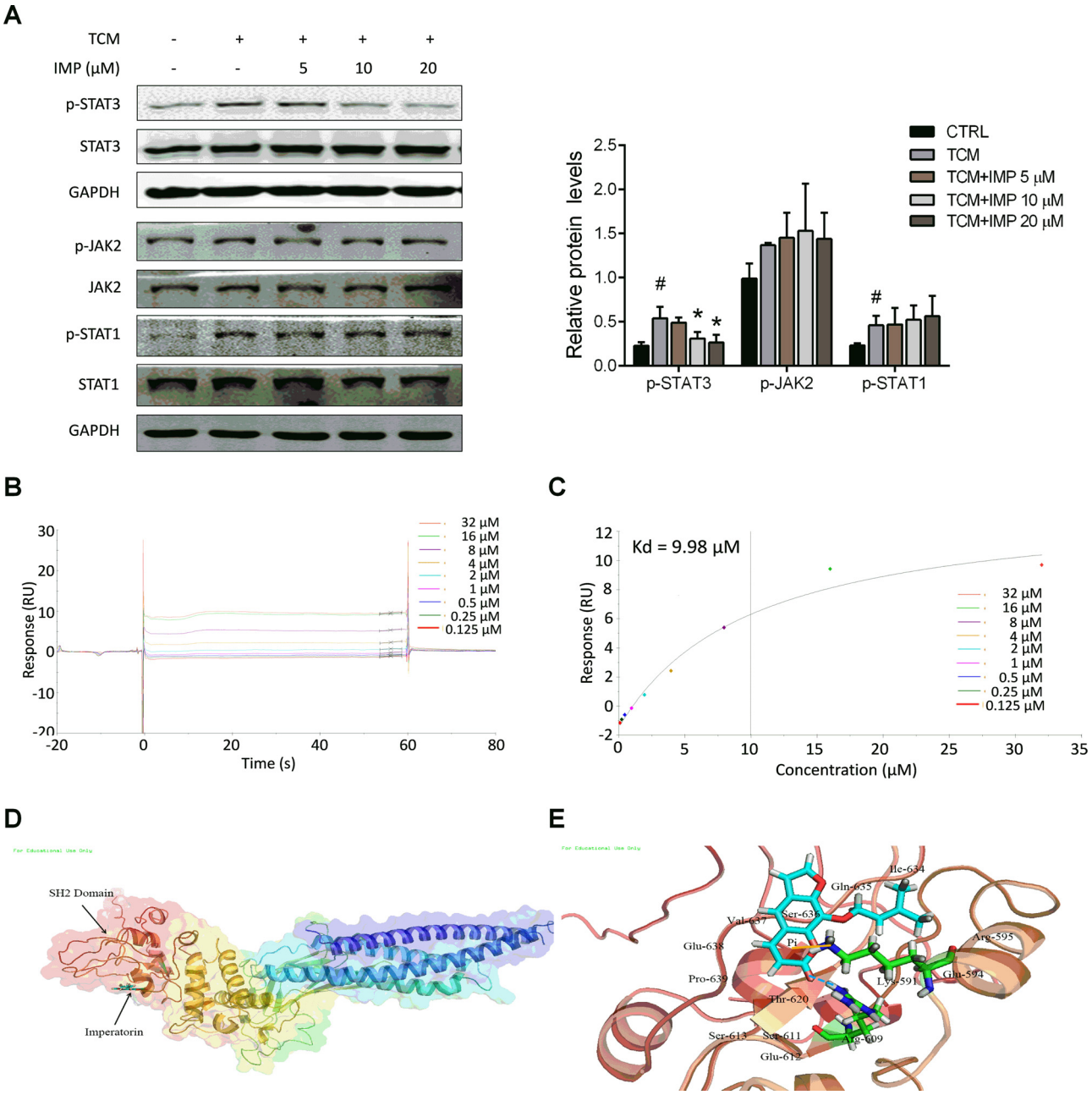

Fig. 6. IMP specifically binds to STAT3. (A) C2C12 myotubes were pretreated with IMP for 2 h and then stimulated by TCM for 15 min. The levels of p-STAT3, p-JAK2 and p-STAT1 were determined by western blot and quantified by densitometry. Total STAT3, JAK2 or STAT1 was used as control. n = 3. $^{\#}P < 0.05$ versus untreated control, $^{*}P < 0.05$ versus TCM control. (B) Dose-response sensorgrams of IMP. (C) The affinity constant K_D values were calculated by global fitting using a steady-state affinity model. (D) Molecular docking analysis of the interaction between IMP and STAT3 SH2 domain. (E) Action modes of IMP with STAT3 SH2 domain.

further concluded that STAT3 mediated the therapeutic effect of IMP on cancer cachexia. The results suggest that IMP may be a promising agent for treatment of cancer cachexia.

Cachexia is a multi-factorial wasting syndrome that not only has a dramatic impact on patient quality of life but also is associated with poor responses to chemotherapy and survival [2,35]. The depletion of skeletal muscle has been accepted as a central event in the development of cancer cachexia and the preservation of muscle mass is considered as a major strategy for anti-cachectic therapy [3,36]. However, the nature of the key players responsible for muscle atrophy in cancer cachexia is still elusive and therapeutic approaches or agents are currently limited [9].

IMP has been shown to possess potential anti-colitis, anti-arthritis and anti-tumor activities [26,27,32]. To investigate the therapeutic effect of IMP on cancer cachexia, we initially evaluated its effect on myotube atrophy induced by TCM and found that IMP dose dependently inhibited myotube atrophy as evidenced by morphological changes and relative fiber width. Meanwhile, the expressions of MuRF1 and Atrogin-1 were also suppressed. *in vivo* experiments, IMP administration strikingly improved the chief features of cancer cachexia in a dose dependent manner, with increased tumor free body weight, gastrocnemius muscle mass, tibialis anterior muscle mass and epididymal fat. Moreover, the myofiber sizes of gastrocnemius muscle were also increased accompanied with decreased expressions of MuRF1 and Atrogin-1. Besides, kidney mass and tumor burden were also improved by IMP treatment at dose of 50 mg/kg. However, the anti-cachexic

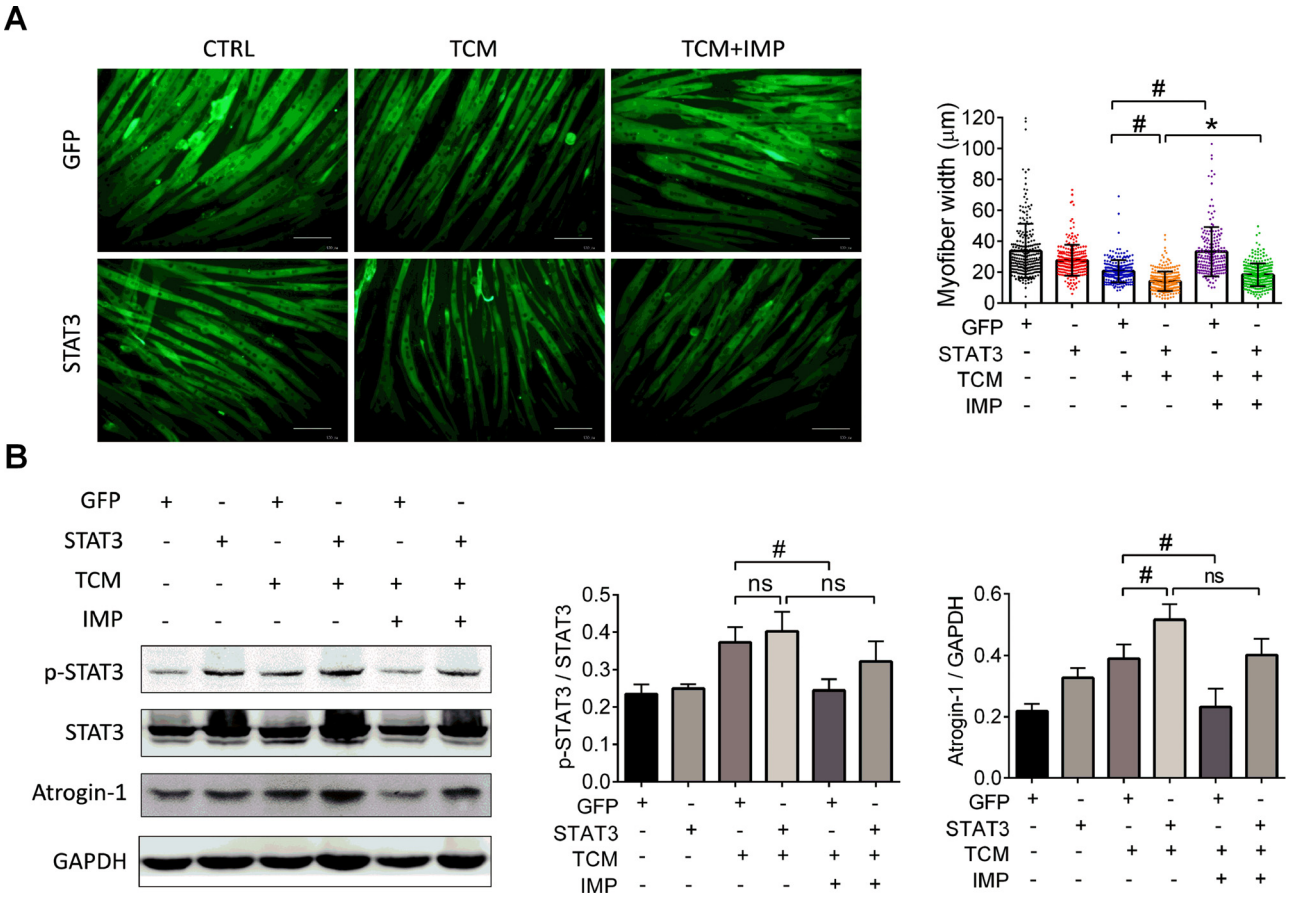

Fig. 7. IMP protects against TCM-induced myotube atrophy via STAT3 inhibition. (A, B) C2C12 myotubes were infected with lentiviruses expressing STAT3 or GFP and then stimulated by TCM for 72 h in the presence of IMP (20 μM) or not. (A) Representative images of immunofluorescence staining for MyHC (green) are shown (left panel). Scale bars = 100 μm. The fiber widths were measured and calculated (right panel). n > 150 per group. $^{\#}P < 0.05$ versus GFP control, $^{*}P < 0.05$ versus TCM control. (B) The expression of indicated proteins was detected by western blot. The band intensities were quantified and total STAT3 or GAPDH was used as control. n = 3. $^{\#}P < 0.05$ versus GFP control, $^{*}P < 0.05$ versus TCM control.

action of IMP seems to be irrelevant to its anti-tumor effect because we observed that IMP (25 mg/kg) prevented cancer cachexia with an insignificant effect on cancer growth. These data demonstrated that IMP could prevent cancer cachexia and improve muscle wasting.

Suppression of excess catabolism by inhibiting protein degradation signaling pathway is an effective mean to prevent skeletal muscle consumption [37]. To elucidate the mechanisms whereby IMP reduces proteolysis, we investigated the effect of IMP on phosphorylation of STAT3, NF-κB, FOXO3 and SMAD2/3, four crucial regulatory pathways of protein degradation [2]. Results showed that IMP only inhibited the phosphorylation of STAT3, which made us mainly focus on STAT3 pathways in the following investigations. Responses to IL-6 stimulations, JAKs are catalytically activated and subsequently mediate tyrosine phosphorylation of STAT3, followed by their dimerization, nuclear translocation, and activation of pro-cachectic genes. To ascertain the direct target of IMP, we analyzed the phosphorylation of JAK2 and STAT1 and found that IMP had no impact on their phosphorylation levels, suggesting that IMP may directly interact with STAT3. This speculation was then confirmed by SPR affinity analysis with binding constants Kd = 9.98 μM. SH2 domain of STAT3 is an important domain which plays key role in STAT3-mediated biological functions and SH2-targeting compounds constitute the largest class of direct STAT3 inhibitor [38]. To evaluate the binding of IMP to the active site of STAT3, molecular docking was performed to calculate the interplay between IMP and SH2 domain of STAT3 by CDOCER in DS 3.0. Results demonstrated that IMP binds to the SH2 domain of STAT3 with a binding energy of -4.7689 kJ/mol. IMP forms a hydrogen bond interaction with Arg-609, and forms a Sigma-Pi interaction with Lys-591.

Though IMP directly interacted with STAT3 and inhibited its phosphorylation, we can still not conclude that IMP improved muscle wasting through STAT3 inhibition. To investigate the mediating effect of STAT3, C2C12 myotubes or gastrocnemius muscles were infected with lentiviruses to overexpress STAT3 and the therapeutic effect of IMP was then evaluated *in vitro* and *in vivo*. Our findings showed that myotube atrophy induced by STAT3 overexpression cannot be reversed by IMP and the inhibitory effect on Atrogin-1 expression was also weakened after STAT3 overexpression. Furthermore, the anti-atrophy effect of IMP in the experimental mouse model of cancer cachexia was also greatly reduced. Thus, we can come to a conclusion that IMP alleviates cancer cachexia and prevents muscle wasting via directly inhibiting STAT3.

However, we have to point out that our investigations mainly focused on muscle tissue or muscle cells and we did not deeply explore the effect of IMP on immune cells and tumor cells or their interactions. Pro-inflammatory cytokines derived from immune or tumor cells, including TNF-α, IL-1 and IL-6, have been shown to trigger muscle wasting in cachexia patients [20]. Our results also showed that IMP inhibited the expression of cytokines (TNF-α, IL-6 and IL-1β) in cachectic muscles (Fig. S4) and decreased the levels of TNF-α and IL-6 in serum of CT26 tumor-bearing mice (data not shown). These findings suggests that IMP has impact on immune or tumor cells, which may explain the observations that anti-atrophy effect of IMP was not completely disappeared after STAT3 overexpression in muscle. But how IMP regulates immune or tumor cells and their interactions with muscle

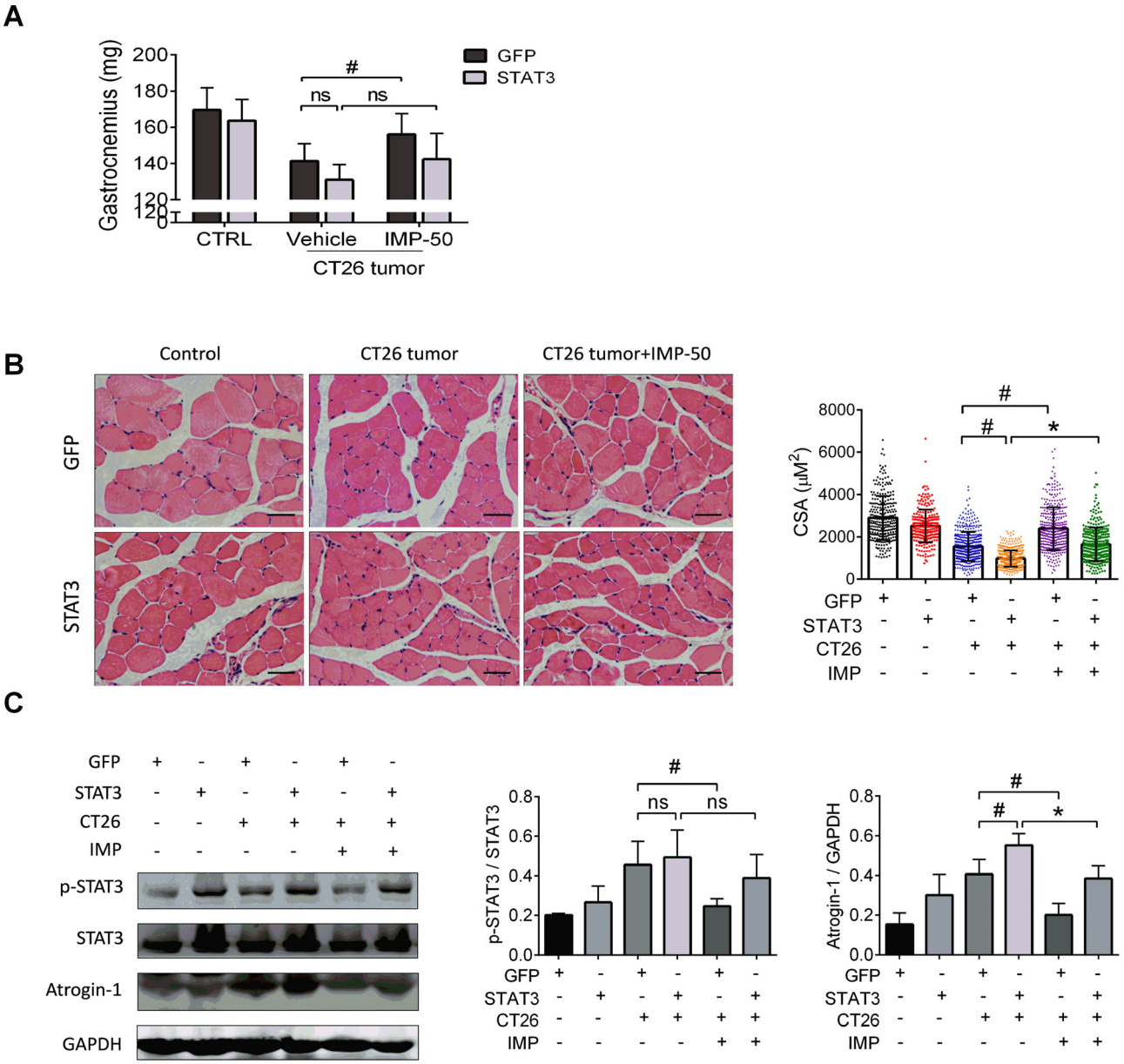

Fig. 8. IMP ameliorates muscle wasting in CT26 tumor-bearing mice through STAT3 inhibition. (A) Average weights of gastrocnemius muscles from both legs of CT26 tumor-bearing mice. (n = 9 mice/group). (B) Gastrocnemius muscle was observed histologically by H&E staining (left panel). Scale bars = 50 μm. The cross-sectional areas of approximately 180 myofibers per group were determined (right panel). n = 3 mice/group. $^{\#}P < 0.05$ versus healthy control, $^{*}P < 0.05$ versus vehicle control. (C) The expression of indicated proteins in gastrocnemius muscles was detected by western blot. The band intensities were quantified and total STAT3 or GAPDH was used as control. n = 3 mice/group. $^{\#}P < 0.05$ versus healthy control, $^{*}P < 0.05$ versus vehicle control.

cells deserves to further investigation.

In summary, we have shown that IMP alleviates cancer cachexia and prevents muscle wasting via directly binding to SH2 domain of STAT3 and inhibiting itself phosphorylation. These findings provide new insights into the therapeutic effect of IMP in cancer cachexia.

Author contribution lists

Cheng Guo and Junping Zhang: designed research and supervised the project.

Cheng Guo and Linlin Chen: drafted the manuscript.

Junping Zhang and Weiheng Xu: modified the manuscript.

Linlin Chen, Weiheng Xu, Quanjun Yang and Hong Zhang: conducted experiments and analyzed data.

Lili Wan and Bo Xin: assisted the animal experiment.

All authors have reviewed and approved the manuscript.

Declaration of Competing Interest

We declare that we have no financial and personal relationships with other people or organizations that can inappropriately influence our work, there is no professional or other personal interest of any nature or kind in any product, service and/or company that could be construed as influencing the position presented in, or the review of the manuscript entitled “Imperatorin alleviates cancer cachexia and prevents muscle wasting via directly inhibiting STAT3″.

Acknowledgments

This work was supported by the National Natural Science Foundation of China (No. 81873042, 81872494) and Shanghai Sailing Program (No. 17YF1424500).

Appendix A. Supplementary data

Supplementary material related to this article can be found, in the online version, at doi:https://doi.org/10.1016/j.phrs.2020.104871.

References

[1] J.M. Argiles, B. Stemmler, F.J. Lopez-Soriano, S. Busquets, Inter-tissue communication in cancer cachexia, Nat. Rev. Endocrinol. 15 (2018) 9–20.
[2] V.E. Baracos, L. Martin, M. Korc, D.C. Guttridge, K.C.H. Fearon, Cancer-associated cachexia, Nat. Rev. Dis. Primers 4 (2018) 17105.
[3] K. Fearon, F. Strasser, S.D. Anker, I. Bosaeus, E. Bruera, R.L. Fainsinger, et al., Definition and classification of cancer cachexia: an international consensus, Lancet Oncol. 12 (2011) 489–495.
[4] L. Martin, L. Birdsell, N. Macdonald, T. Reiman, M.T. Clandinin, L.J. McCargar, et al., Cancer cachexia in the age of obesity: skeletal muscle depletion is a powerful prognostic factor, independent of body mass index, J. Clin. Oncol. 31 (2013) 1539–1547.
[5] X. Zhou, J.L. Wang, J. Lu, Y. Song, K.S. Kwak, Q. Jiao, et al., Reversal of cancer cachexia and muscle wasting by ActRIIB antagonism leads to prolonged survival, Cell 142 (2010) 531–543.
[6] T.S. Bowen, V. Adams, S. Werner, T. Fischer, P. Vinke, M.N. Brogger, et al., Small-molecule inhibition of MuRF1 attenuates skeletal muscle atrophy and dysfunction in cardiac cachexia, J. Cachexia Sarcopenia Muscle 8 (2017) 939–953.
[7] T.J. Wright, E.L. Dillon, W.J. Durham, A. Chamberlain, K.M. Randolph, C. Danesi, et al., A randomized trial of adjunct testosterone for cancer-related muscle loss in men and women, J. Cachexia Sarcopenia Muscle 9 (2018) 482–496.
[8] E.T. Pring, G. Malietzis, R.H. Kennedy, T. Athanasiou, J.T. Jenkins, Cancer cachexia and myopenia - Update on management strategies and the direction of future research for optimizing body composition in cancer - A narrative review, Cancer Treat. Rev. 70 (2018) 245–254.
[9] A. Molfino, M.I. Amabile, A. Giorgi, M. Monti, V. D'Andrea, M. Muscaritoli, Investigational drugs for the treatment of cancer cachexia: a focus on phase I and phase II clinical trials, Expert Opin. Investig. Drugs 28 (2019) 733–740.
[10] L. Zhang, J. Pan, Y. Dong, D.J. Tweardy, Y. Dong, G. Garibotto, et al., Stat3 activation links a C/EBPdelta to myostatin pathway to stimulate loss of muscle mass, Cell Metab. 18 (2013) 368–379.
[11] J.F. Ma, B.J. Sanchez, D.T. Hall, A.K. Tremblay, S. Di Marco, I.E. Gallouzi, STAT3 promotes IFNgamma/TNFalpha-induced muscle wasting in an NF-kappaB-dependent and IL-6-independent manner, EMBO Mol. Med. 9 (2017) 622–637.
[12] K.A. Silva, J. Dong, Y. Dong, Y. Dong, N. Schor, D.J. Tweardy, et al., Inhibition of Stat3 activation suppresses caspase-3 and the ubiquitin-proteasome system, leading to preservation of muscle mass in cancer cachexia, J. Biol. Chem. 290 (2015) 11177–11187.
[13] W.A. He, E. Berardi, V.M. Cardillo, S. Acharyya, P. Aulino, J. Thomas-Ahner, et al., NF-kappaB-mediated Pax7 dysregulation in the muscle microenvironment promotes cancer cachexia, J. Clin. Invest. 123 (2013) 4821–4835.
[14] D. Cai, J.D. Frantz, N.E. Tawa Jr, P.A. Melendez, B.C. Oh, H.G. Lidov, et al., IKKbeta/NF-kappaB activation causes severe muscle wasting in mice, Cell 119 (2004) 285–298.
[15] C.M. Op den Kamp, R.C. Langen, F.J. Snepvangers, C.C. de Theije, J.M. Schellekens, F. Laugs, et al., Nuclear transcription factor kappa B activation and protein turnover adaptations in skeletal muscle of patients with progressive stages of lung cancer cachexia, Am. J. Clin. Nutr. 98 (2013) 738–748.
[16] A. Rebbapragada, H. Benchabane, J.L. Wrana, A.J. Celeste, L. Attisano, Myostatin signals through a transforming growth factor beta-like signaling pathway to block adipogenesis, Mol. Cell. Biol. 23 (2003) 7230–7242.
[17] J.L. Chen, K.L. Walton, A. Hagg, T.D. Colgan, K. Johnson, H. Qian, et al., Specific targeting of TGF-beta family ligands demonstrates distinct roles in the regulation of muscle mass in health and disease, Proc Natl Acad Sci U S A 114 (2017) E5266–e5275.
[18] M. Sandri, C. Sandri, A. Gilbert, C. Skurk, E. Calabria, A. Picard, et al., Foxo transcription factors induce the atrophy-related ubiquitin ligase atrogin-1 and cause skeletal muscle atrophy, Cell 117 (2004) 399–412.
[19] M. Sandri, J. Lin, C. Handschin, W. Yang, Z.P. Arany, S.H. Lecker, et al., PGC-1alpha protects skeletal muscle from atrophy by suppressing FoxO3 action and atrophy-specific gene transcription, Proc Natl Acad Sci U S A 103 (2006) 16260–16265.
[20] K.C. Fearon, D.J. Glass, D.C. Guttridge, Cancer cachexia: mediators, signaling, and metabolic pathways, Cell Metab. 16 (2012) 153–166.
[21] T. Mori, T. Miyamoto, H. Yoshida, M. Asakawa, M. Kawasumi, T. Kobayashi, et al., IL-1beta and TNFalpha-initiated IL-6-STAT3 pathway is critical in mediating inflammatory cytokines and RANKL expression in inflammatory arthritis, Int. Immunol. 23 (2011) 701–712.
[22] F.E. Marino, G. Risbridger, E. Gold, Activin-betaC modulates cachexia by repressing the ubiquitin-proteasome and autophagic degradation pathways, J. Cachexia Sarcopenia Muscle 6 (2015) 365–380.
[23] O. Rom, A.Z. Reznick, The role of E3 ubiquitin-ligases MuRF-1 and MAFbx in loss of skeletal muscle mass, Free Radic. Biol. Med. 98 (2016) 218–230.
[24] A. Sukari, I. Muqbil, R.M. Mohammad, P.A. Philip, A.S. Azmi, F-BOX proteins in cancer cachexia and muscle wasting: emerging regulators and therapeutic opportunities, Semin. Cancer Biol. 36 (2016) 95–104.
[25] S.C. Bodine, E. Latres, S. Baumhueter, V.K. Lai, L. Nunez, B.A. Clarke, et al., Identification of ubiquitin ligases required for skeletal muscle atrophy, Science 294 (2001) 1704–1708.
[26] M. Liu, G. Zhang, C. Zheng, M. Song, F. Liu, X. Huang, et al., Activating the pregnane X receptor by imperatorin attenuates dextran sulphate sodium-induced colitis in mice, Br. J. Pharmacol. 175 (2018) 3563–3580.
[27] K.F. Zhai, H. Duan, Y. Chen, G.J. Khan, W.G. Cao, G.Z. Gao, et al., Apoptosis effects of imperatorin on synoviocytes in rheumatoid arthritis through mitochondrial/caspase-mediated pathways, Food Funct. 9 (2018) 2070–2079.
[28] Y.Z. Li, J.H. Chen, C.F. Tsai, W.L. Yeh, Anti-inflammatory property of imperatorin on alveolar macrophages and inflammatory lung injury, J. Nat. Prod. 82 (2019) 1002–1008.
[29] X. Li, X. Zeng, J. Sun, H. Li, P. Wu, K.P. Fung, et al., Imperatorin induces Mcl-1 degradation to cooperatively trigger Bax translocation and Bak activation to suppress drug-resistant human hepatoma, Cancer Lett. 348 (2014) 146–155.
[30] M. Assi, F. Derbre, L. Lefeuvre-Orfila, A. Rebillard, Antioxidant supplementation accelerates cachexia development by promoting tumor growth in C26 tumor-bearing mice, Free Radic. Biol. Med. 91 (2016) 204–214.
[31] Q. Yang, L. Wan, Z. Zhou, Y. Li, Q. Yu, L. Liu, et al., Parthenolide from Parthenium integrifolium reduces tumor burden and alleviate cachexia symptoms in the murine CT-26 model of colorectal carcinoma, Phytomedicine 20 (2013) 992–998.
[32] C. Mi, J. Ma, K.S. Wang, H.X. Zuo, Z. Wang, M.Y. Li, et al., Imperatorin suppresses proliferation and angiogenesis of human colon cancer cell by targeting HIF-1alpha via the mTOR/p70S6K/4E-BP1 and MAPK pathways, J. Ethnopharmacol. 203 (2017) 27–38.
[33] L. Chen, D. Lv, X. Chen, M. Liu, D. Wang, Y. Liu, et al., Biosensor-based active ingredients recognition system for screening STAT3 ligands from medical herbs, Anal. Chem. 90 (2018) 8936–8945.
[34] S. Becker, B. Groner, C.W. Müller, Three-dimensional structure of the Stat3beta homodimer bound to DNA, Nature 394 (1998) 145–151.
[35] S.M. Kazemi-Bajestani, V.C. Mazurak, V. Baracos, Computed tomography-defined muscle and fat wasting are associated with cancer clinical outcomes, Semin. Cell Dev. Biol. 54 (2016) 2–10.
[36] E.C.W. Neefjes, R.M. van den Hurk, S. Blauwhoff-Buskermolen, M. van der Vorst, A. Becker-Commissaris, M.A.E. de van der Schueren, et al., Muscle mass as a target to reduce fatigue in patients with advanced cancer, J. Cachexia Sarcopenia Muscle 8 (2017) 623–629.
[37] Y. Miyamoto, D.L. Hanna, W. Zhang, H. Baba, H.J. Lenz, Molecular pathways: cachexia signaling-a targeted approach to Cancer treatment, Clin. Cancer Res. 22 (2016) 3999–4004.
[38] B.D. Page, D.P. Ball, P.T. Gunning, Signal transducer and activator of transcription 3 inhibitors: a patent review, Expert Opin. Ther. Pat. 21 (2011) 65–83.